

Supporting Information

Experimental and Theoretical Identification of Heptavalent Fe(VII) Oxidation State in FeO_4^-

Jun-Bo Lu,^{a†} Jiwen Jian,^{b†} Wei Huang,^a Hailu Lin,^b Jun Li^{a*}, Mingfei Zhou^{b*}

Calculation Results

Geometric optimizations were performed on various possible structures of FeO_4^- by using Gaussian 09. The optimized structural parameters of the four lowest-lying structures at the B3LYP level are shown in Figure 3 in the article. Structure **A** is a tetroxide with a 2A_1 ground state and a slightly distorted tetrahedral structure of D_{2d} symmetry. The four Fe=O bond are equivalent with a bond length of 160.4 pm. Structure **B** has a 2A_2 ground state with C_{2v} symmetry, which involves a side-on bonded peroxide ligand and a bent OFeO dioxide fragment. The two Fe-O bonds have a bond length of 179.1 pm and the two Fe=O bonds have a bond distance of 158.9 pm. The O-O bond with a bond length of 143.5 pm is a typical peroxide ligand. Structure **C** has a 6B_1 ground state with C_{2v} symmetry involving a side-on bonded superoxide ligand with an O-O bond length of 133.1 pm. The Fe-O bond lengths are 210.0 pm and the two Fe=O bond distances are 164.7 pm. The fourth structure (**D**) has a 6A_1 ground state with D_{2d} symmetry, which involves two equivalent side-on bonded peroxide ligands with an O-O bond distance of 149.4 pm.

The vibrational frequencies and intensities of the D_{2d} symmetry tetroxide FeO_4^- and the C_{2v} symmetry $[(\eta^2\text{-O}_2)\text{FeO}_2]^-$ calculated at various DFT levels are given in Tables S1 and S2. The relative energies of the four FeO_4^- isomers calculated at various DFT levels and at the CCSD(T) level are listed in Table S3. Testing calculations showed that with extra diffusion functions similar results were obtained.

Table S1. Calculated vibrational frequencies (cm⁻¹) and intensities (in parentheses in km/mol) of the D_{2d} symmetry tetroxide FeO₄⁻ (Structure **A** in Figure 3).

B3LYP		TPSSh		M06L		PBE	
¹⁶ O	¹⁸ O						
911.2(265)	873.6(243)	941.9(374)	903.1(344)	911.0(171)	875.1(155)	897.3(156)	862.0(142)
903.3(183)	867.3(167)	920.0(174)	883.8(159)	881.5(206)	844.7(189)	868.4(193)	832.4(177)
884.6(0)	833.7(0)	880.8(0)	830.4(0)	862.2(0)	812.8(0)	842.5(0)	794.2(0)
396.6(1)	379.0(1)	390.1(1)	372.7(1)	392.3(1)	374.9(1)	378.4(1)	361.5(1)
361.7(0)	341.0(0)	362.0(0)	341.3(0)	354.6(0)	334.3(0)	351.2(0)	331.1(0)
338.3(0)	319.0(0)	330.5(0)	311.5(0)	326.0(0)	307.3(0)	318.7(10)	305.2(9)
336.9(10)	322.5(8)	327.1(10)	313.2(8)	321.3(16)	307.8(13)	317.1(0)	298.9(0)

Table S2. Calculated vibrational frequencies (cm⁻¹) and intensities (in parentheses in km/mol) of the C_{2v} symmetry [(η²-O₂)FeO₂]⁻ (Structure **B** in Figure 3).

B3LYP		TPSSh		M06L		PBE	
¹⁶ O	¹⁸ O						
987.2(163)	941.0(148)	981.4(156)	935.1(146)	972.9(160)	925.4(155)	951.1(142)	905.0(137)
964.3(343)	926.4(314)	960.9(174)	923.0(290)	942.0(301)	904.6(275)	868.4(193)	885.3(255)
954.0(1)	901.1(0.3)	944.4(4)	892.8(0)	939.4(11)	889.3(1)	913.2(10)	864.6(2)
590.1(5)	565.1(4)	606.3(7)	580.2(5)	600.3(11)	574.8(8)	594.2(10)	568.7(7)
490.9(20)	465.5(18)	486.3(20)	461.3(18)	483.5(19)	459.5(17)	436.5(17)	414.0(15)
333.5(1)	315.5(0)	323.6(1)	306.2(0)	331.4(1)	313.5(0)	320.2(0)	303.0(0)
247.9(0)	233.7(0)	242.0(0)	228.1(0)	255.2(0)	240.6(0)	237.0(0)	223.4(0)
236.2(3)	225.4(2)	229.1(3)	218.7(2)	237.8(3)	227.1(2)	223.2(3)	213.1(2)
221.9(21)	214.4(18)	225.0(17)	217.4(14)	235.7(11)	227.3(9)	221.2(10)	213.8(8)

Table S3. Relative energies (in kcal/mol) of different FeO₄⁻ isomers calculated at various DFT levels and at the CCSD(T) and CASPT2 level (The T₁ and D₁ diagnostic values are also listed).*

Isomer	OS	B3LYP	TPSSh	M06L	PBEPBE	CCSD(T)	CASPT2	T ₁	D ₁
FeO ₄ ⁻ (A)	VII	5.9	0	0	0	0	0	0.09	0.35
[(η ² -O ₂)Fe ^{VO} O ₂] ⁻ (B)	V	0	2.6	14.9	16.6	2.3	19.91	0.05	0.17
[(η ² -O ₂)Fe ^{IV} O ₂] ⁻ (C)	IV	5.1	14.7	28.2	43.2	14.4	-	0.06	0.19
[Fe(η ² -O ₂) ₂] ⁻ (D)	III	24.9	33.4	53.7	69.9	30.0	-	0.05	0.17

* The active space for CASPT2 includes Fe: 3d and O: 2p, i.e., CAS(25_e,17_o)

Table S4. The configuration and coefficients of FeO_4^- and $[(\eta^2\text{-O}_2)\text{Fe}^{\text{V}}\text{O}_2]^-$ from CAS(25e, 17o)-SCF.

FeO_4^-		$[(\eta^2\text{-O}_2)\text{Fe}^{\text{V}}\text{O}_2]^-$	
Configuration	Coefficient	Configuration	Coefficient
2222a022202220220	0.7402755	222202220220022a	0.8114299
2222a022202220202	-0.1045014	222202220202022a	-0.1911704
2222a022202220022	-0.0834496	220220222022022a	-0.1200733
2222a022022220220	-0.0787872	2222202202220022a	-0.0894352
2222a022202202220	-0.0787868	22222220220220022a	-0.0759893
2222a022202220b2a	-0.071361	2222022220220022a	-0.0737885
2220a222202220220	-0.0646545	222220222202aa022b	-0.0697289
222baa22202220220	0.0587601	222220222ba22002a2	0.0684319
2222a022202020222	-0.0581526	2222ba2b2a220022a	0.067405
2222a020202220222	-0.0581514	2222ba22ab220022a	-0.0647612
222220a2202b2022a	0.0541712	2222ab22ba220022a	-0.0642977
2222202b20a22022a	-0.0541701	2ba220222022ab22a	-0.0637674
222baa22202220a2b	-0.0539675	2222ba222022002a2	-0.0633011
2222a022202a2b2ba	0.052824	2220202222220022a	-0.0606393
2222a02a2b22202ba	0.052822	222b2b2a2a220022a	-0.0596737
2222a0222022ba220	0.0525437	2222ab2a2b220022a	0.0591661
2222a022ba2220220	0.0525432	222220222202ba022a	0.0589569
222aab22202220b2a	-0.0518739	222a2a2b2b220022a	-0.0583835
2222b022202220a2a	0.0518255	222220222ba220022a	0.0573309
2a2220222022ba220	-0.0517386	222b2a22ba220022a	-0.0572414
2a222022ba2220220	-0.0517357	2ab220222022ba22a	-0.0552164
2222a022202220220	0.7402755	22222a2b20a200222	-0.0550442
2222a022202220202	-0.1045014	222220222ab22002a2	-0.0539673
2222a022202220022	-0.0834496	2222ba2220220022a	-0.0539044
2222a022022220220	-0.0787872	222b2a2b2a220022a	0.052896
2222a022202202220	-0.0787868	222a2b22ab220022a	-0.0523083
2222a022202220b2a	-0.071361	2bb220222022aa22a	0.05173
2220a222202220220	-0.0646545	2222ab222022002a2	0.0507489
		22222022220220022a	0.8114299
		22222022220202022a	-0.1911704
		2202202220220222a	-0.1200733
		2222202202220022a	-0.0894352
		22222220220220022a	-0.0759893
		2222022220220022a	-0.0737885

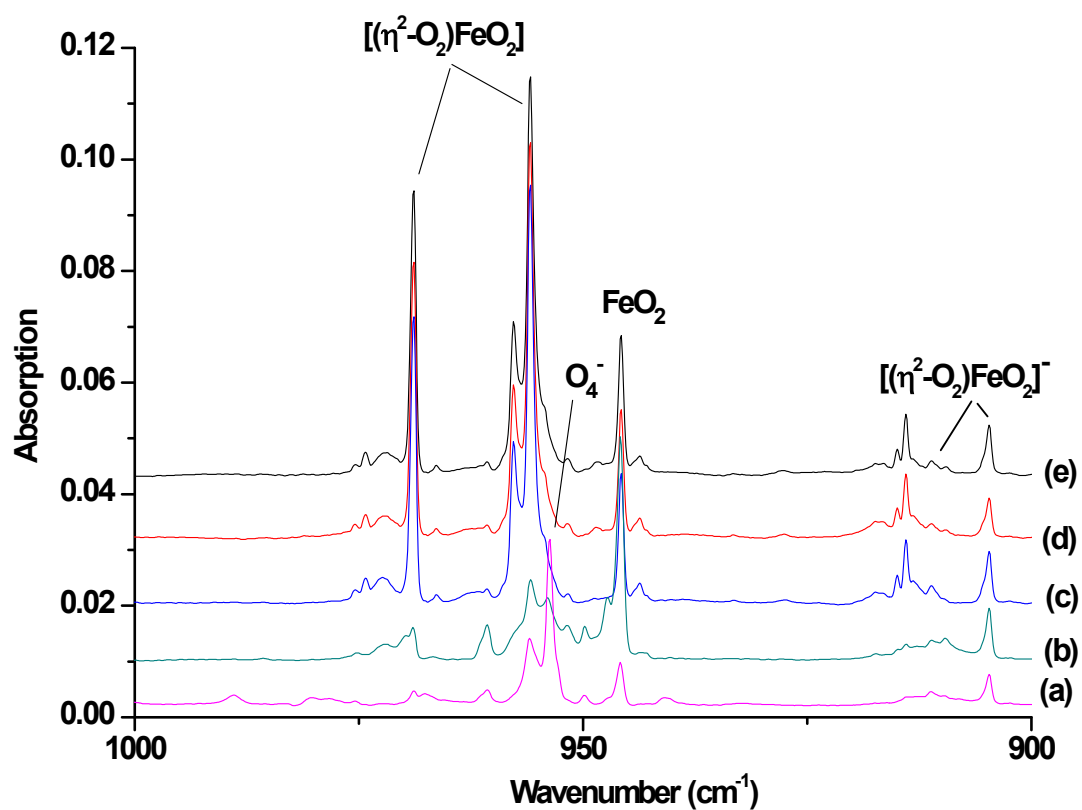


Figure S1. Infrared spectra in the 1000-900 cm⁻¹ region from co-deposition of laser-evaporated iron atoms and electrons with 2.0 % O₂ in solid argon. (a) after 1 h of sample deposition at 4 K, (b) after 15 min of UV light irradiation (250 λ <math>< 580</math> nm), (c) after annealing to 28 K, (d) after 15 min of visible light irradiation (500 λ <math>< 580</math> nm), and (e) after 15 min of UV-visible light irradiation (280 λ <math>< 580</math> nm).

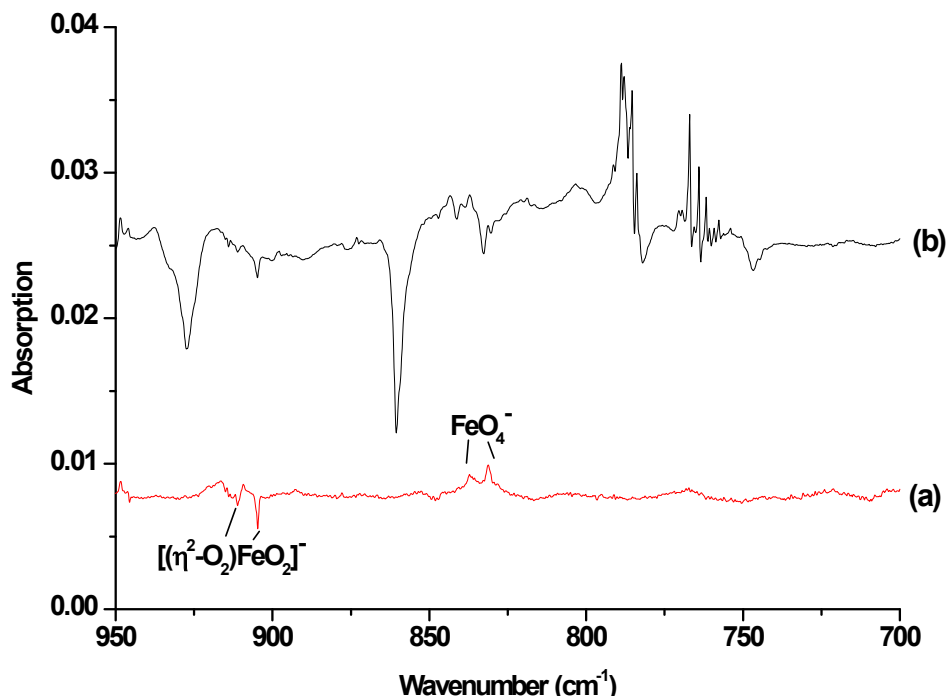


Figure S2. Infrared spectra in the 950-700 cm^{-1} region from co-deposition of Fe with different gas mixtures (spectra taken after 15 min of $\lambda > 500$ nm light irradiation minus spectrum after 28 K annealing). (a) 2 % O_2 in argon , (b) 2 % O_2 + 0.1 % CCl_4 in argon.

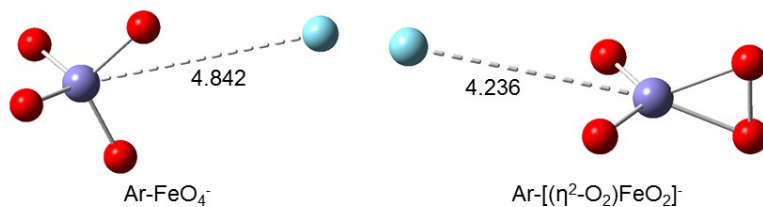


Figure S3. The optimized geometry structures of Ar-FeO_4^- and $\text{Ar-}[(\eta^2\text{-O}_2)\text{FeO}_2]^-$

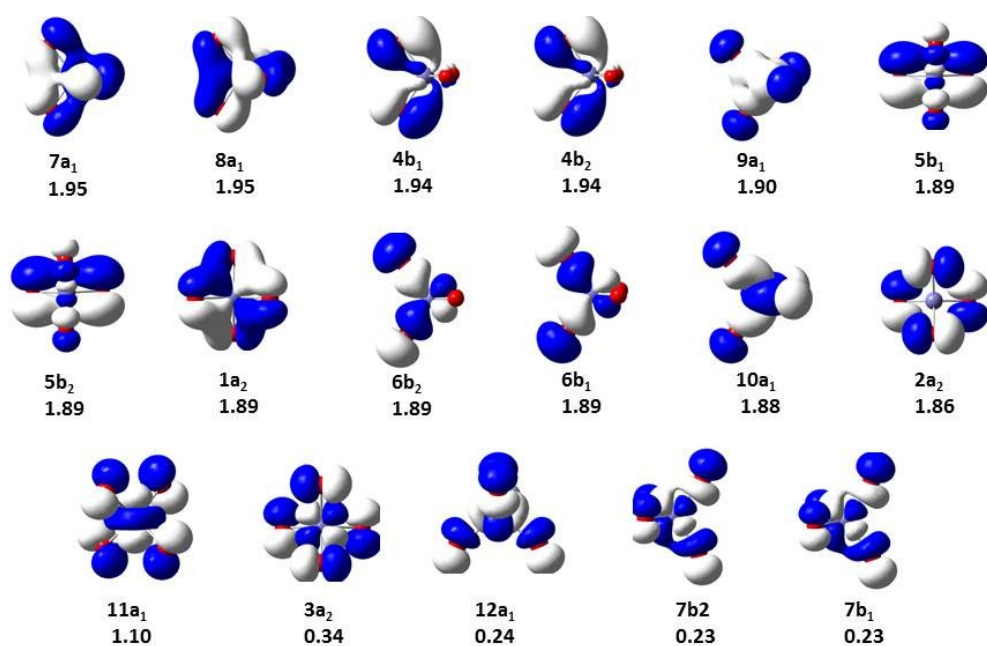


Figure S4. FeO₄²⁻ natural valence orbitals with occupation numbers from CAS(25_e,17_o)-SCF calculations.

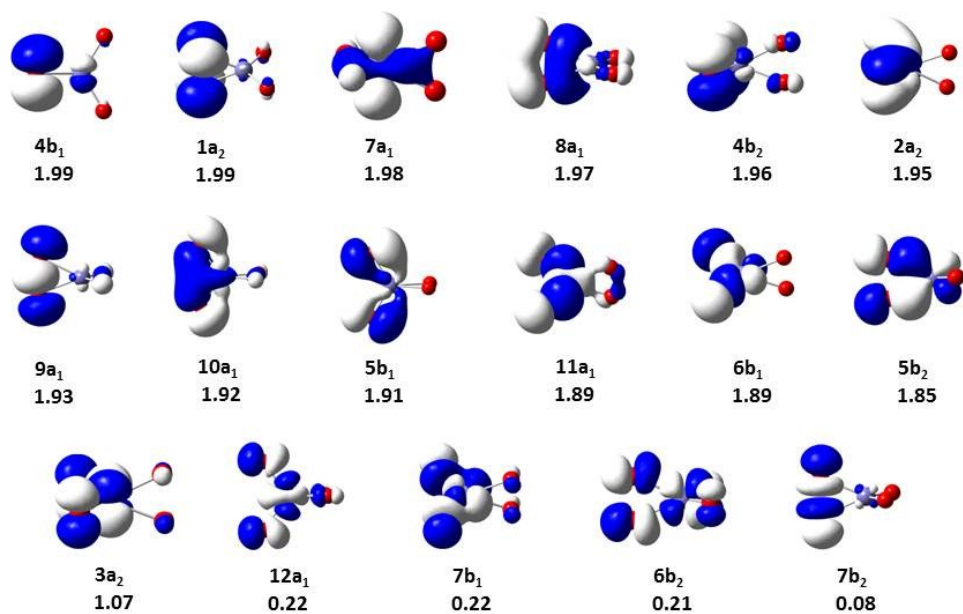


Figure S5. [(η²-O₂)FeO₂]⁻ natural valence orbitals with occupation numbers from CAS(25_e,17_o)-SCF calculations.

Selection of Active Spaces and Energies of DMRG Calculations

As discussed in the article, from the DMRG-CASCI natural orbitals of the two isomers **A** and **B**, we can conclude that the oxidation states of **A** and **B** are VII and V, respectively. From In our calculations, the DMRG-CASCI calculations need huge active space to obtain reasonable results. For CAS4, the energy gap between the two isomers is 4.58 kcal/mol. When further dynamic correlation is included, a slight change of relative energy occurs. For the DMRG-CASSCF-NEVPT2 calculations, the energy gap of two isomers is about 7.54 kcal/mol for CAS1. We can conclude that the two isomers are nearly degenerate when we add the Fe:4d orbitals into the active space from the result of DMRG-CASSCF-NEVPT2 calculations with CAS2. By inspecting the orbitals in the active space, it appears that some of the Fe 4d orbitals and O 3p orbitals also contribute to the strong static correlation.

Table S5. DMRG-CASCI energy (in Hartree) versus discarded weight of the FeO_4^- and $[(\eta^2\text{-O}_2)\text{FeO}_2]^-$ for different types of active space.

Active Space	M	FeO_4^-			$[(\eta^2\text{-O}_2)\text{FeO}_2]^-$		
		OS	Discarded weight	Energy	OS	Discarded weight	Energy
CAS(18o, 25e)	1000		1.214×10^{-4}	-1570.87885		2.814×10^{-5}	-1570.88405
	2000		2.846×10^{-4}	-1570.88058		7.886×10^{-6}	-1570.88436
	3000	VII	8.122×10^{-6}	-1570.88086	V	2.676×10^{-6}	-1570.88439
	3500		4.661×10^{-6}	-1570.88089		1.606×10^{-6}	-1570.88440
	∞		-	-1570.88102		-	-1570.88444
CAS(23o, 25e)	1000		3.390×10^{-4}	-1571.00321		2.208×10^{-4}	-1571.02469
	2000		2.137×10^{-4}	-1571.01558		1.046×10^{-4}	-1571.02852
	3000	VII	1.625×10^{-4}	-1571.02035	V	6.267×10^{-5}	-1570.02965
	3500		1.412×10^{-4}	-1571.02187		5.128×10^{-5}	-1571.02995
	∞		-	-1571.04198		-	-1571.03163
CAS(26o, 25e)	1000		8.065×10^{-4}	-1571.10836		1.165×10^{-4}	-1571.14667
	2000		5.030×10^{-4}	-1571.12961		5.465×10^{-5}	-1571.15194
	3000	VII	3.435×10^{-4}	-1571.13864	V	3.587×10^{-5}	-1571.15308
	3500		2.922×10^{-4}	-1571.14134		3.075×10^{-5}	-1571.15340
	∞		-	-1571.16084		-	-1571.15340
CAS(42o, 25e)	1000		5.710×10^{-4}	-1571.32717		1.307×10^{-4}	-1571.38345
	1500		3.759×10^{-4}	-1571.35922		1.042×10^{-4}	-1571.39046
	2000	VII	4.552×10^{-4}	-1571.34749	V	9.01×10^{-5}	-1571.39433
	2500		3.398×10^{-4}	-1571.36844		8.124×10^{-5}	-1571.39690
	∞		-	-1571.42612		-	-1571.41881

Table S6. DMRG-CASCI-SC-NEVPT2 energy (in Hartree) of the FeO_4^- and $[(\eta^2\text{-O}_2)\text{FeO}_2]^-$

Orbital number	FeO_4^-		$[(\eta^2\text{-O}_2)\text{FeO}_2]^-$	
	OS	Energy	OS	Energy
CAS (18o, 25e)	VII	-1572.68179	V	-1572.65604
CAS (23o, 25e)		-1572.60410		-1572.59127

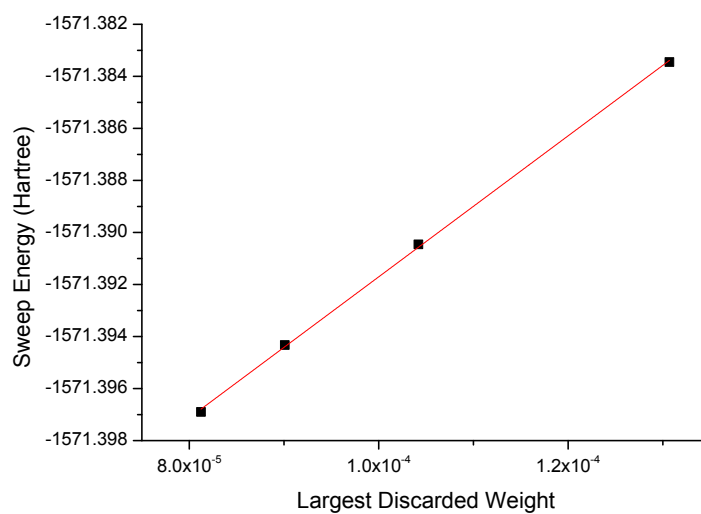


Figure S6. DMRG-CAS(25_e, 41_o)-CI energy versus discarded weight of $[(\eta^2\text{-O}_2)\text{FeO}_2]^-$.

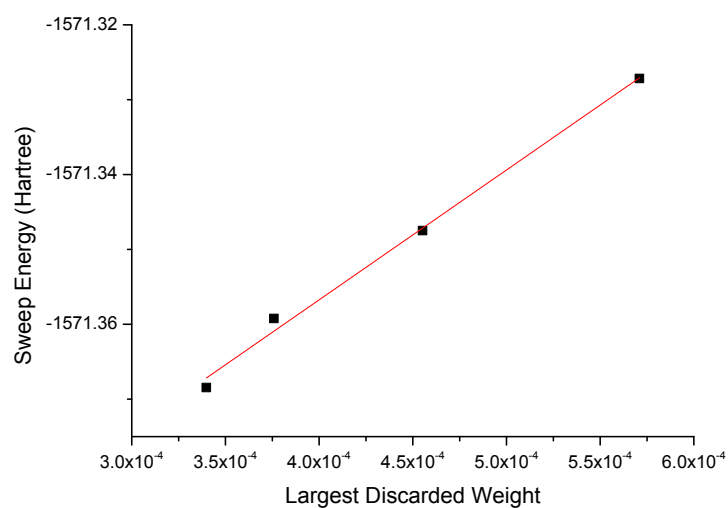


Figure S7. DMRG-CAS(25_e, 41_o)-CI energy versus discarded weight of FeO_4^- .

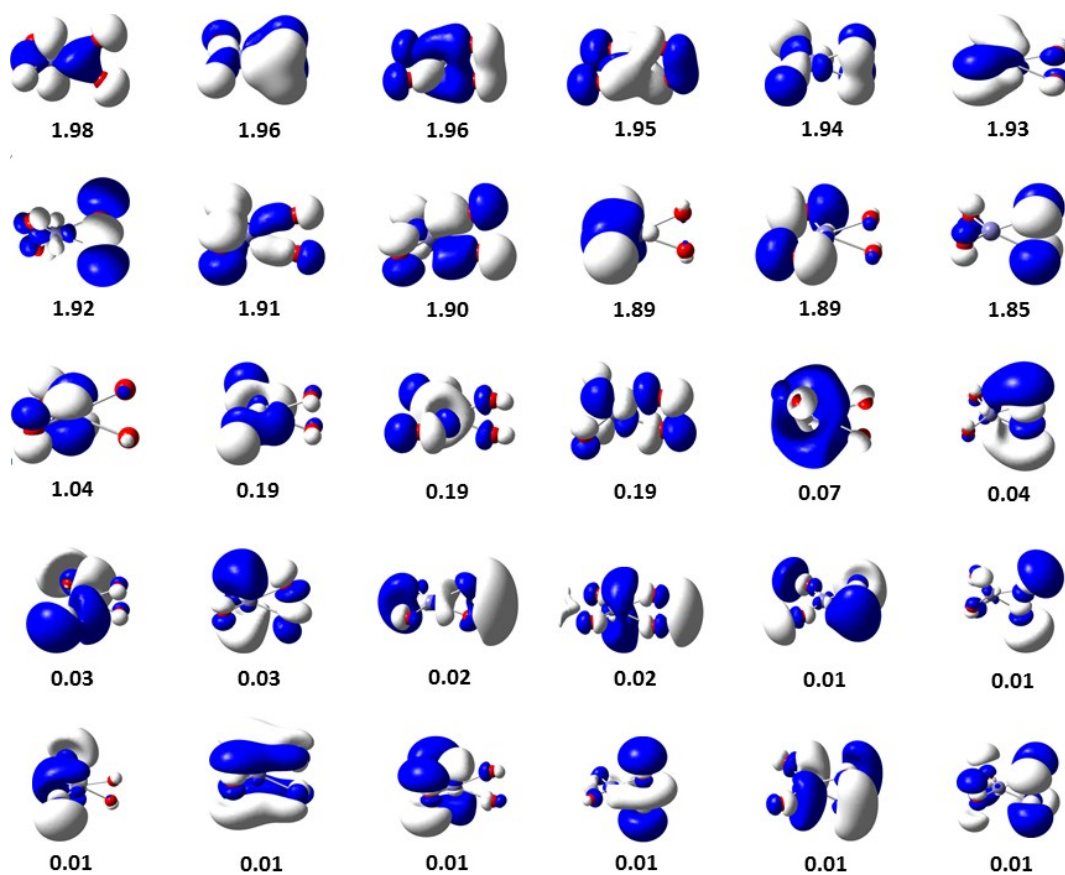


Figure S8. DMRG-CAS(25_e,42_o)-CI natural orbitals (with occupation numbers than 0.01) of $[(\eta^2\text{-O}_2)\text{FeO}_2]$.

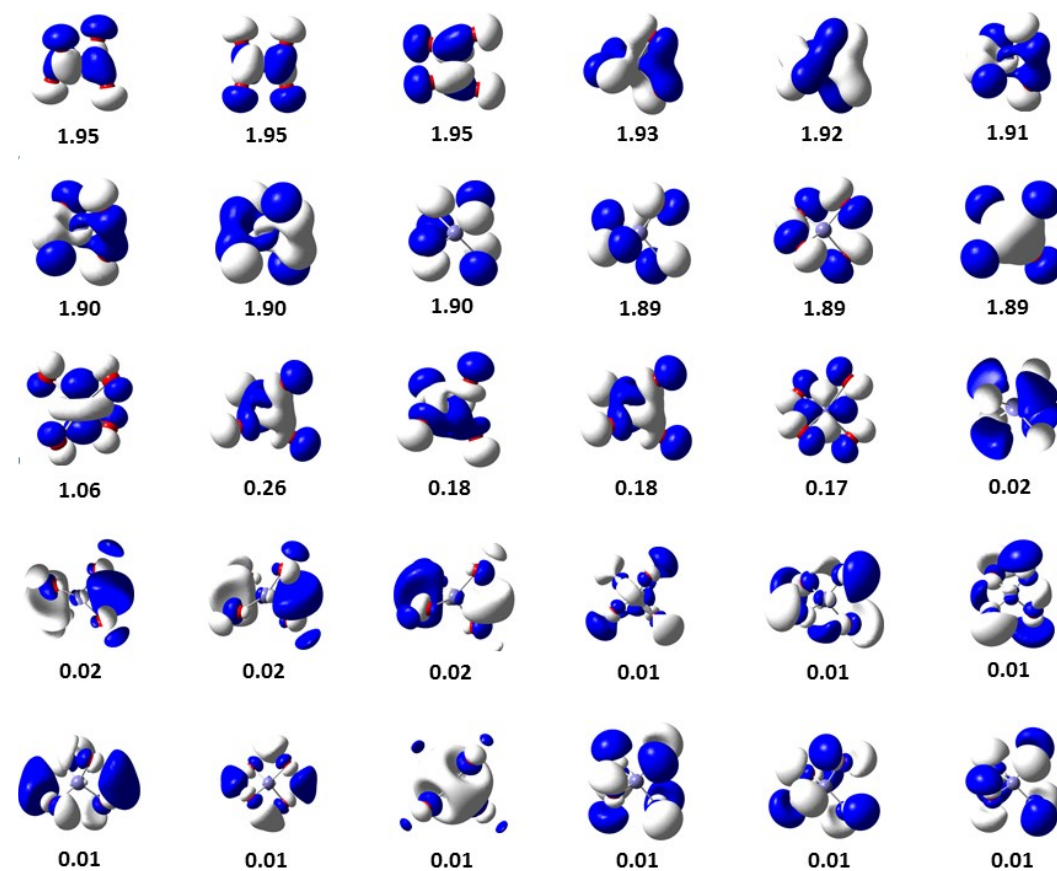


Figure S9. DMRG-CAS(25_e,42_o)-CI natural orbitals (with occupation numbers than 0.01) of FeO_4^- .

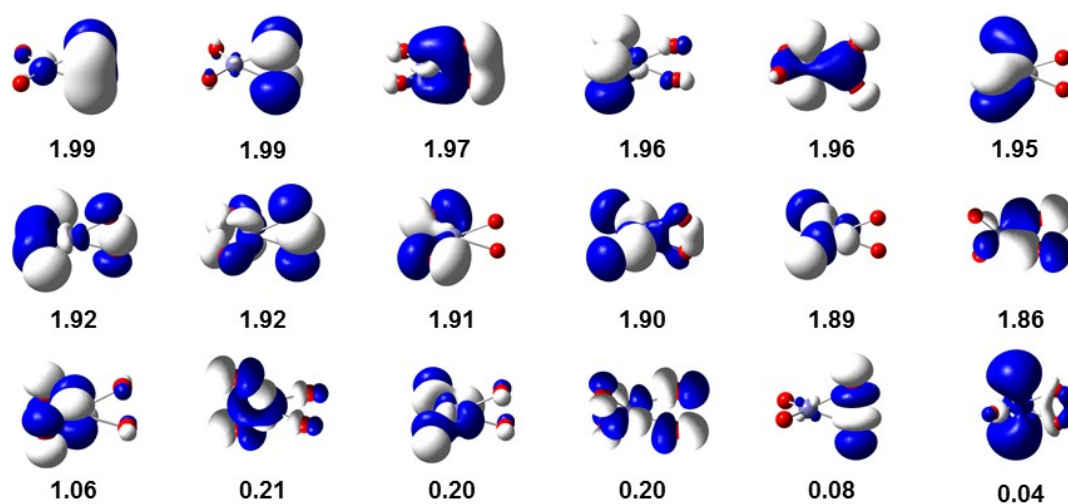


Figure S10. DMRG-CAS(25_e,18_o)-SCF natural orbitals (with occupation numbers) of $[(\eta^2\text{-O}_2)\text{FeO}_2]$.

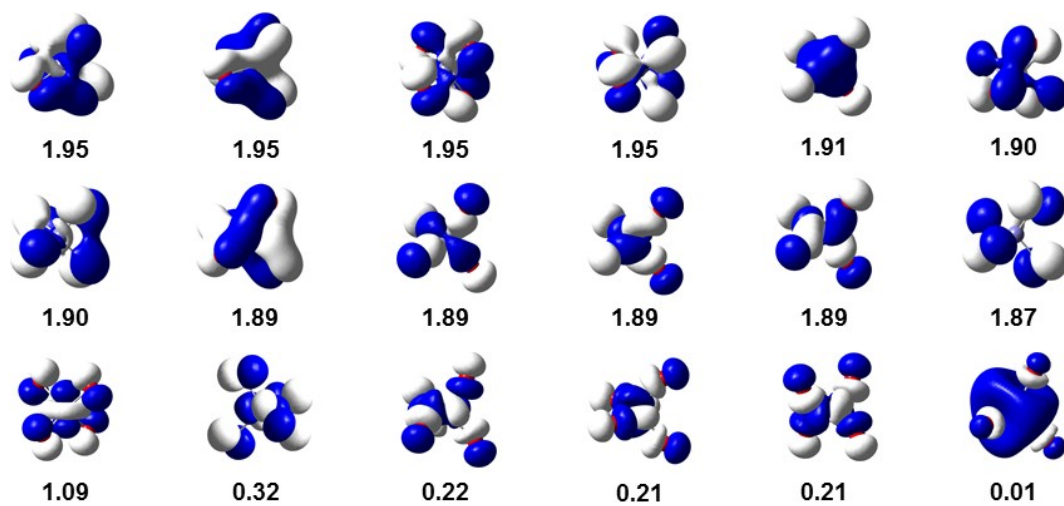


Figure S11. DMRG-CAS(25_e,18_o)-SCF natural orbitals (with occupation numbers) of FeO_4 .

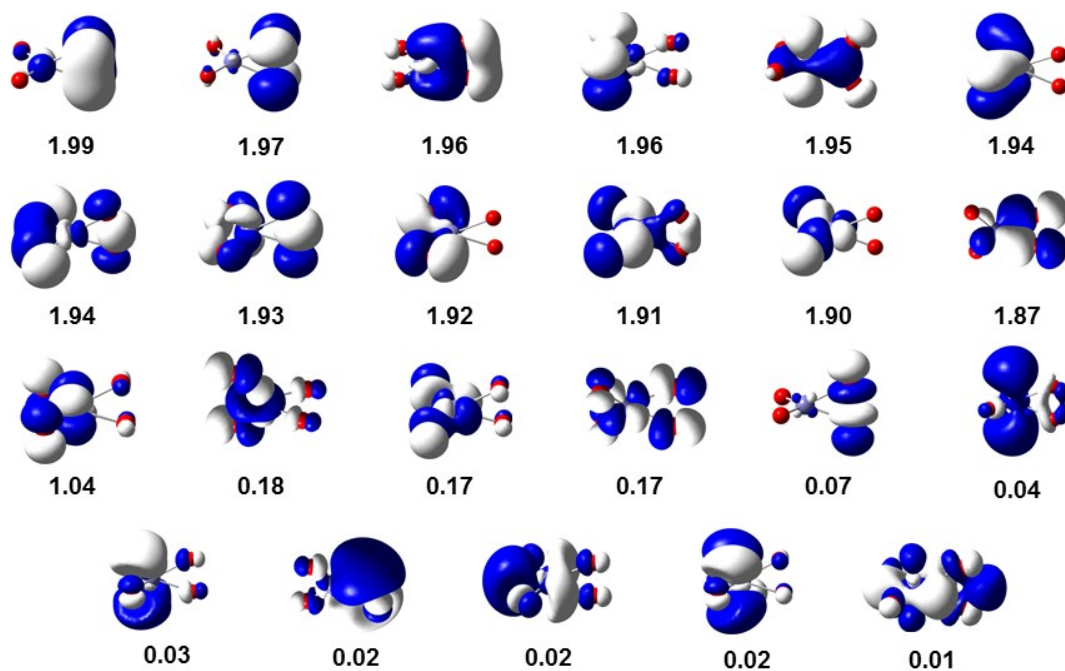


Figure S12. DMRG-CAS(25_e,23_o)-SCF natural orbitals (with occupation numbers) of $[(\eta^2\text{-O}_2)\text{FeO}_2]$.

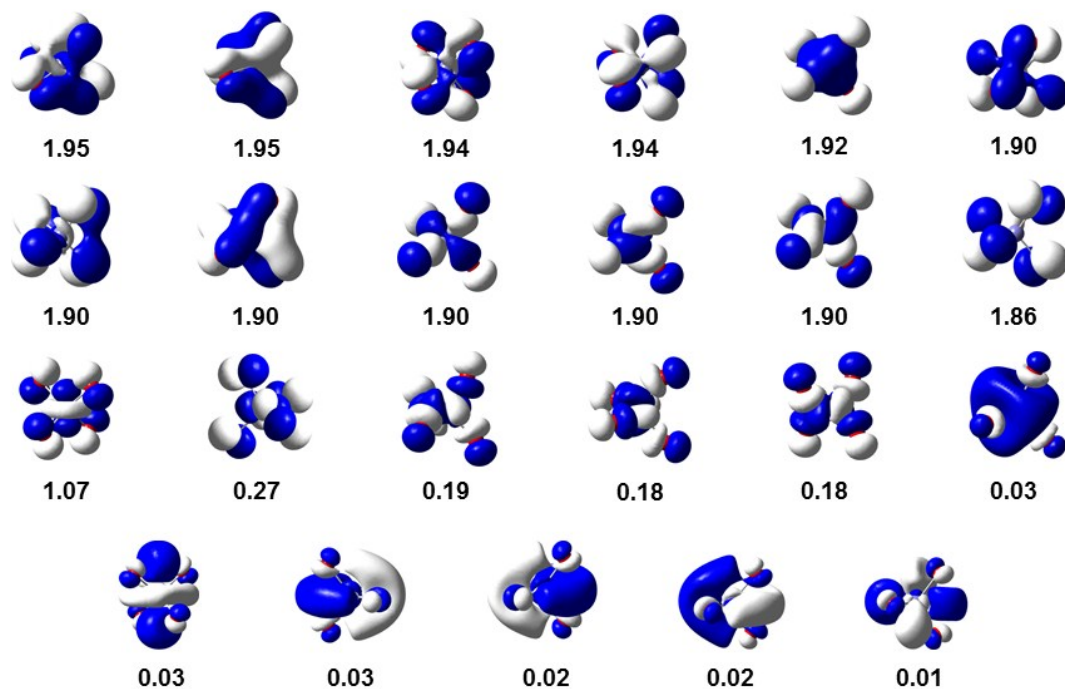


Figure S13. DMRG-CAS(25_e,23_o)-SCF natural orbitals (with occupation numbers) of FeO_4 .

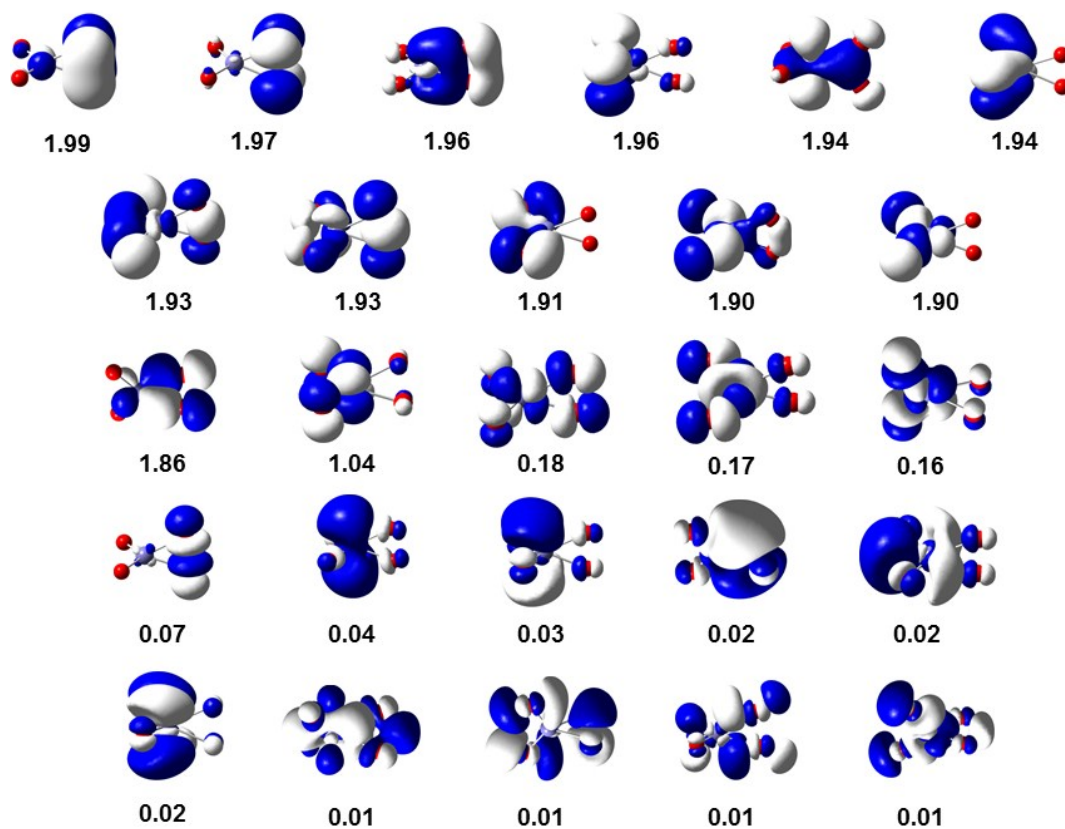


Figure S14. DMRG-CAS(25_e,26_o)-SCF natural orbitals (with occupation numbers) of $[(\eta^2\text{-O}_2)\text{FeO}_2]$.

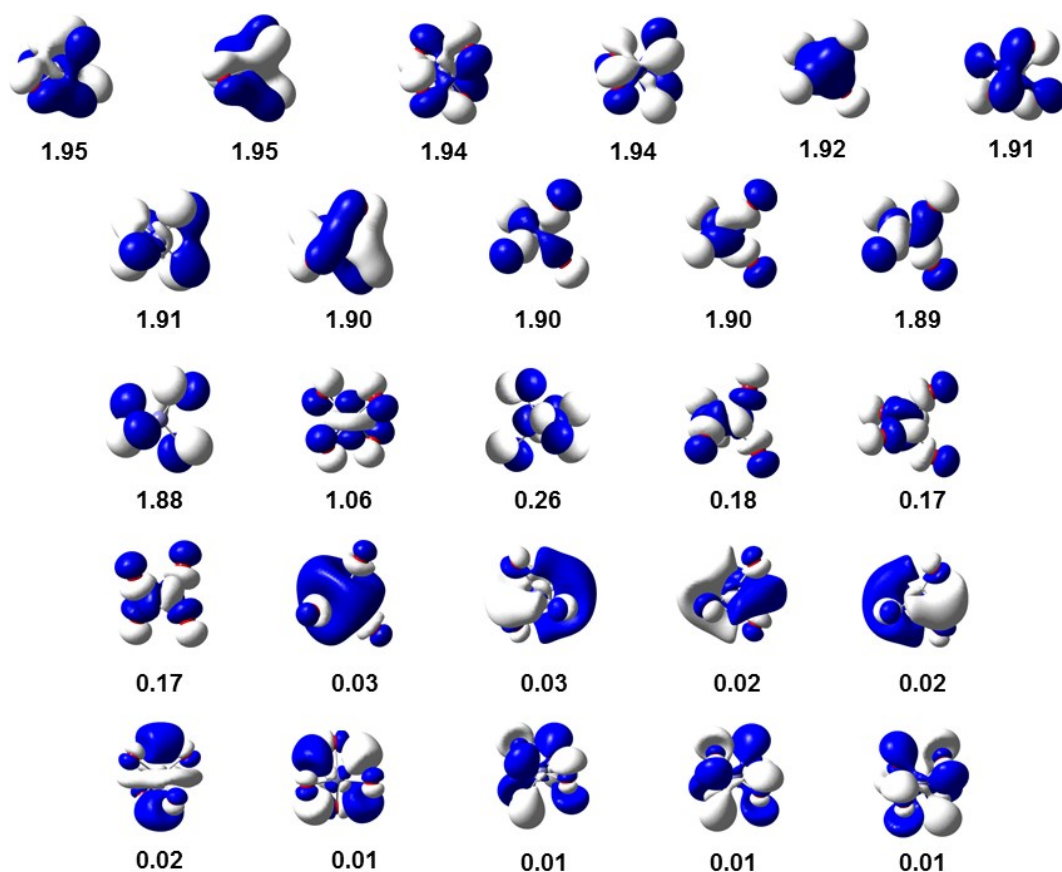


Figure S15. DMRG-CAS(25_e,26_o)-SCF natural orbitals (with occupation numbers) of FeO₄⁻.

Table S7. DMRG-CASSCF and DMRG-CASSCF-SC-NEVPT2 energies (in Hartree) of the FeO₄⁻ and [(η²-O₂)FeO₂]⁻.

Orbital number	FeO ₄ ⁻			[(η ² -O ₂)FeO ₂] ⁻		
	OS	DMRG-CASSCF	MR-PT [†]	OS	DMRG-CASSCF	MR-PT [†]
CAS1		-1571.19691	-1572.63852		-1571.19319	-1572.63480
CAS2	VII	-1571.35097	-1572.63517	V	-1571.35916	-1572.63313
CAS3		-1571.44314	-		1571.42867	-

[†]MR-PT is DMRG-CASSCF-SC-NEVPT2

Linear Transit

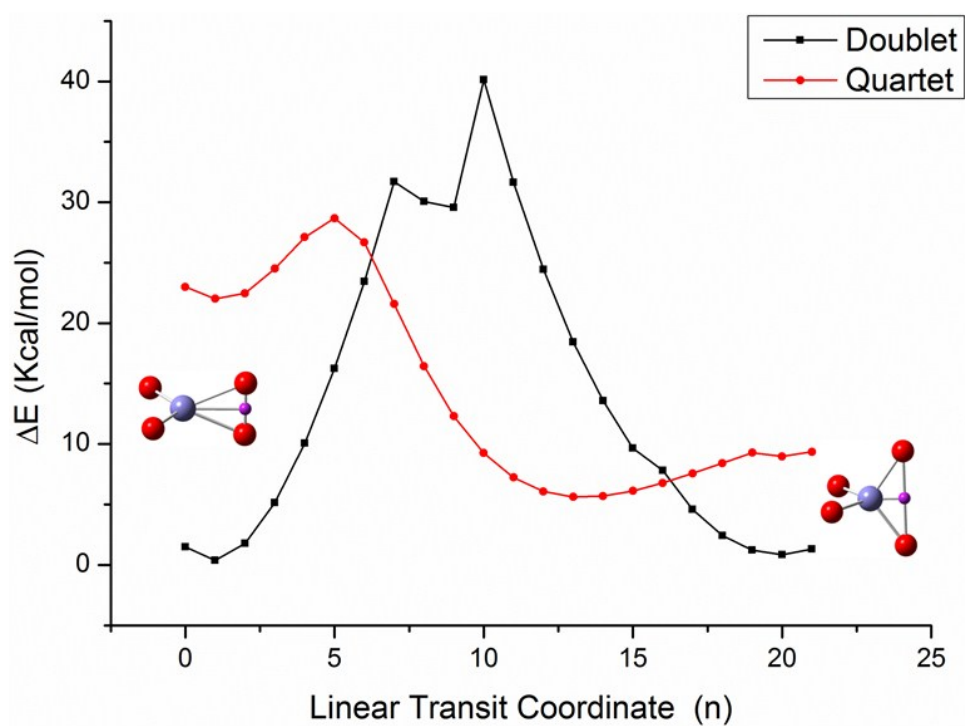


Figure S16. Linear synchronous transit (LST) energy curves obtained by SR-DFT/B3LYP calculations, illustrating the transitions between $[(\eta^2\text{-O}_2)\text{Fe}^{\text{VO}_2}]^-$ (quartet) and $\text{Fe}^{\text{VII}}\text{O}_4^-$ (doublet) upon change of distance (R_n) from Fe to the center of $\eta^2\text{-O}_2$, where $R_n = R_0 - 0.0375n$, with starting point $R_1=1.644 \text{ \AA}$ and ending point $R_{20}=0.932 \text{ \AA}$.